European Online Journal of Natural and Social Sciences 2014; www.european-science.com
Vol.3, No.3 Special Issue on Environmental, Agricultural, and Energy Science
ISSN 1805-3602

Optimization of Horizontal Axis wind Turbine Airfoil by Using the Inverse Panel

Milad Babadi Soultanzadeh*, Babak Mehmandoost Esfahani
Department of Mechanical Engineering, Khomeini Shahr branch, Islamic Azad University, Khomeini Shahr, Iran
*Email: milad.babadi@iaukhsh.ac.ir

Abstract

In this paper we studied the optimization of NACA 4412 which is one of the widely used airfoils in the wind energy industry in the horizontal axis wind turbines working at low Reynolds numbers and low-speed winds. Since these turbines require high torque to start working, optimization is done by inverse design panel based on increasing lift force. Assuming stability of upper level, three different designs of speed distribution were applied to the lower level and changes to the primary airfoil geometry resulted from a few repetitions. Then, by direct panel method and CDF modeling and using Spalart-Allmaras turbulent model, aerodynamic loads on designed airfoils are predicted. Also, the impact of the number of panels on accuracy of results is analyzed. Finally, results are compared with experimental aerodynamic characteristics of the primary airfoils. For all projects, the lift coefficient and the ratio of lift to drag at all angles of attack were greater than the initial airfoil and the accuracy of the new optimized airfoil is confirmed for working in low Reynolds numbers.

Keywords: renewable energy, wind turbine, airfoil design, panel method, CFD, Spalart-Allmaras

Introduction

With increasing concerns about the environment, research about environmentally friendly renewable energy sources increased. Focus on these resources is due to increased environmental pollution (chemical and thermal pollution), increasing global energy demand and declining fossil energy resources. Renewable energy includes solar, biomass, geothermal, hydroelectric and wind. Wind energy is one of the energies that provide a variety of choices for researchers. This energy currently has the fastest growth rate among other renewable resources (Babadi, et al. 2014).

Airfoil is one of the basic parts of the wind turbine blade designs. Aerodynamic characteristics of rotor significantly depend on the airfoil-shaped blades. Purpose and efficiency of airfoil is to create a low pressure area over the blades to generate lift force, also the drag force is produced unintentionally (Singh, et al., 2012). Although, the performance of wind turbines is affected by the three-dimensional flow and the non-permanent factors, significant achievements can be made by designing, improving and choosing proper airfoil (Henriques, 2009).

The impact of Atmosphere Boundary Layer (ABL) is low in the height at which wind turbines are usually installed and the wind is almost calm. Atmosphere Boundary Layer (ABL) depends on the topology and the surface roughness. If turbines work in urban areas or areas with rough surface, wind speed is reduced under the atmospheric boundary layer influence (Yao, 2012). For example, in urban areas the average wind speed is less than the summer areas and mountains. With regard to advances in wind systems and their more economization, main concerns in these conditions is the issue of starting to work and annually producing more energy of a renewable resource (Henriques, 2009).

Good aerodynamic performance of airfoil is the key factor which greatly influences work startup and performance coefficient of wind turbines[4]. Airfoil families NACA 44XX ،NACA

23XXX ،NACA 63-XXX ،Wortmann FX are airfoils that are traditionally used in wind turbines (Tangler, & Somers, 1995).

So far, airfoil design traditionally follows three methods: first, direct design based on trial and error, second, inverse design resulted from computer advance and numerical codes and third; changes in airfoil geometry. In the present study, changes in the geometry of the available airfoils (Singh, et al, 2012 & Henriques, et al. 2009 & Rajakumar & Ravindran, 2012) are used. At low speed winds for high startup torque, high lift is required. Experiences show that the S-shaped lower surface, especially in the circuit volatile edge leads to increase in lift force. In this study, NACA 4412 airfoil is considered as the initial geometry. As a result, by the changing geometry of the lower surface NACA 4412 in S form at the volatile edge, the 4412 lift can be raised. The geometry of the airfoil with design method panel is Changed by the XFOIL code (Drela, n.d.). So that, the new velocity distribution (pressure distribution) on the airfoil resulting from the underside of the new S shape is applied to the initial airfoil and new geometry can be achieved after a few repetitions. Then, the new airfoil lift and drag coefficients are predicted in two numerical methods of direct panel and CFD and performance coefficient charts are calculated for each airfoil. This is done for three different speed distribution schemes and the results were compared with each other and the initial airfoil. Figure (1) shows the initial NACA 4412 airfoil and the new optimized airfoil.

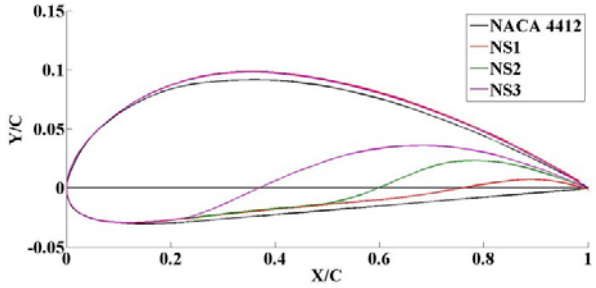

Figure 1. Airfoil Geometry and Optimized Airfoils

Panel Method

Panel method was first proposed by Hess-Smith in 1962 with Neumann Boundary Condition and based on flat panel with Constant source of power. This method was first applied for non-lift flows but was analyzed with doublet instead of lift spring issues (Kamoun, et al. 2005). By developing computers and numerical codes in next years, panel methods was proposed with boundary conditions and different panels. In this research, Linear-vorticity stream function Panel method was used. In the inverse method, 160 panels were used on the primary airfoil level and then the impact of the number of panels on the results was analyzed directly.

However, the panel method is only capable of analyzing non-slimy flows. For incompressible non-slimy flows, Navier-Stoks equation will be turned into Laplace Equation (Moran, 1984).

$$\nabla^2 \phi = 0 \qquad (1)$$

In equation (1), ϕ is the potential of flow rate. Since this is the partial differential equation of the second convention, the sum of any particular solution of this equation is a particular solution to this equation. As a result, unlike CFD methods, in the panel method it is not necessary to solve the flow field around the objects in question, rather only by determining the strength of single panels by the help of the zero speed perpendicular on the surface, the speed tangent to the surface, distribution of pressure on the surface and finally aerodynamic loads can be calculated (Katz & Plotkin, 1991).

After simplifications, in direct method panel locations were first identified and then distribution of speed and pressure for each panel is obtained by solving linear equation system, although in inverse method, speed distribution on primary surface was first identified and then the panel locations were calculated.

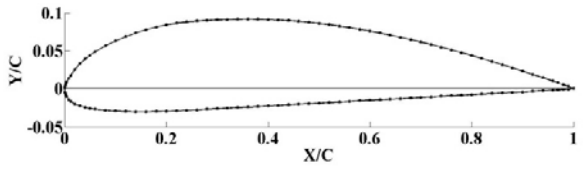

Figure 2. Paneling Primary Airfoils for Inverse Design Method

Results of reverse design show that; although new speed distribution is only applied on the lower level of primary airfoil, after doing calculations a high level has also been minimally changed. The numbers of repetitions for convergence of NS1 ،NS2 و NS3 were respectively 3, 4, 4. After obtaining new geometry, the new direct method was applied for lift and drag coefficients. Also, the effect of the number of panels for predicting lift coefficient of primary airfoil is shown in 4 degree angle of attack in figure 3.

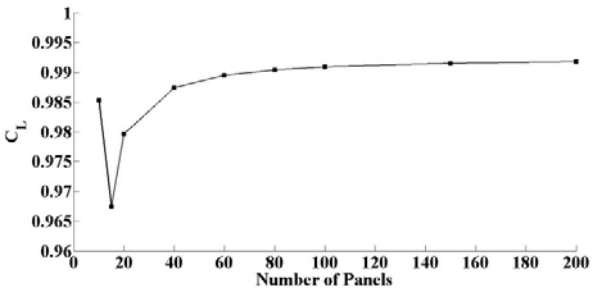

Figure 3. Changes of Lift Coefficient Dependent on the Number of Panels in 4 Degree Angle Of Attack (NACA 4412)

CFD Modeling

In order to predict the wind turbine behavior, the aerodynamic loads and the flow field around it are analyzed (Bhutta, et al. 2012). Also, it is so important in simulating these problems to pay attention to the flow complexities like Dynamic Stall three-dimensional vortex. Empirical tests of wind tunnel can help a better understanding of aerodynamic wind turbines but requires much equipment and cost for it. Also, results should be obtained so that measurement equipment does not influence the orbit circuit significantly and these results should be processed for post processing. Instead, computational fluid dynamics methods can give detailed characteristics about flow without using complex systems, also they enable us to have regular studies like parametric analysis on the system performance without spending too much (Li, C., et al. 2013).

In the meanwhile, Turbulence Model plays an important role in modeling CFD turbulent flows. Prediction of turbulent flows phenomenon such as boundary layer depends heavily on applied turbulent model (Deck, et al., 2002). Spalart-Allmaras is a single equation model that is frequently used in aerodynamic problems (Allmaras, et al., 2012). This model compared to double-equation models such as $K-\varepsilon$ are less sensitive to deterioration of the computational grid and for flows with Adverse Pressure Gradient provide good results (Pramod, 2011 & Ravi, et al, 2013). Since wind

turbines keep working in stall conditions analysis of aerodynamic loads on wind turbine airfoils under boundary layer separation conditions (Kang, et al., 2013)created by adverse pressure Gradient) and stall is so important. As a result, Spalart-Allmaras can be an appropriate turbulent model for modeling CFD flow around wind turbine airfoil.

Solved equations for flow are Navier-Stocks equations by buffering which are solved by turbulent model equation in couple form. Equation (2) is continuity equation. Equation (3) is the averaged Reynolds Navier-Stocks equation in Tensorial form for Steady State. The R_{ij} statement is called Reynolds Stress Tensor and its value is stated by equation (4). ‹x ‹P ρ‹ and υ are speed, spatial component, density and kinematic viscosity. υ_t is effective turbulent kinematic viscosity.

$$\frac{\partial u_i}{\partial x_i} = 0 \tag{2}$$

$$u_j \frac{\partial u_i}{\partial x_j} = -\frac{1}{\rho}\frac{\partial P}{\partial x_i} + \upsilon \nabla^2 u_i - \frac{\partial R_{ij}}{\partial x_j} \tag{3}$$

$$R_{ij} = -\upsilon_t \left(\frac{\partial u_i}{\partial x_j} + \frac{\partial u_j}{\partial x_i}\right) \tag{4}$$

$$\frac{\partial}{\partial x_i}(\rho \tilde{\upsilon} u_i) = G_\upsilon + \frac{1}{\sigma_\upsilon}\left\{\begin{array}{l} \dfrac{\partial}{\partial x_j}\left[(\mu + \rho\tilde{\upsilon})\dfrac{\partial \tilde{\upsilon}}{\partial x_j}\right] \\ +C_{b2}\rho\left(\dfrac{\partial \tilde{\upsilon}}{\partial x_j}\right)^2 \end{array}\right\} + Y_\upsilon + S_{\tilde{\upsilon}} \tag{5}$$

Equation (5) is partial differential equation to find turbulent viscosity. $\tilde{\upsilon}$ is the same as turbulent kinematic viscosity that turn into effective kinematic viscosity by multiplying in a coefficient in the equation (4). For more information and awareness of equation coefficients and constants refer to [14], [18], [19]. For gridding square solution tetrahedral cells were used. Figure (4) shows gridding square solution and near airfoil network for NS3. Gridding around airfoils are so fine and in the flow area under the partition influence a little coarse and after that in the open circuit is a little more coarse. The network independence is studied and the results confirm stability with a little change less than 2%. CDF modeling is conducted for angles of attack between 0 to 20 with 2 degree step and lift and drag coefficients determine the distribution of pressure coefficient on airfoils. Since the chord length of airfoils is one meter, (8) and (6) equations explain lift and drag coefficients. In these equations, C_P, C_D, C_L are pressure, drag and lift coefficients respectively.

$$C_L = \frac{L}{\frac{1}{2}\rho V_\infty^2} \tag{6}$$

$$C_D = \frac{D}{\frac{1}{2}\rho V_\infty^2} \tag{7}$$

$$C_P = \frac{P - P_\infty}{\frac{1}{2}\rho V_\infty^2} \tag{8}$$

L ‹D ‹P ‹P_∞ and V_∞ are lift force, drag force, airfoil pressure and free esteem pressure and free esteem velocity. Bellow the CFD modeling conditions are represented:

Spalart-Allmaras turbulent model was used.

Weather was assumed as ideal gas.

Viscosity is fixed fluid.
Equations are solved at steady state.
Pressure-velocity coupling was used for SIMPLE algorithm.
Standard Wall Function was used near airfoil wall.

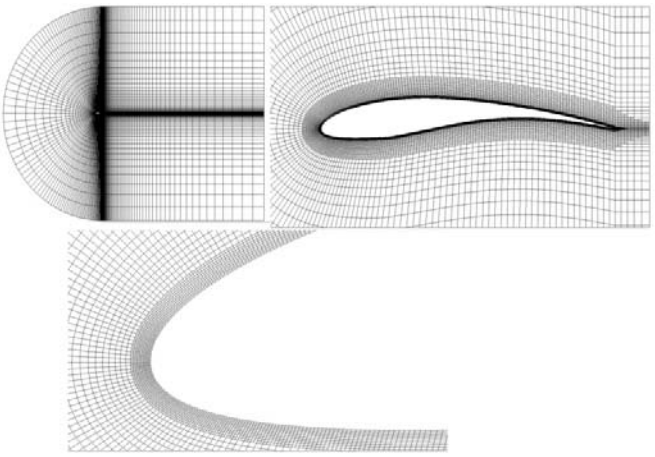

Figure 4. Gridding Square Solution CDF

Results and Discussion

CFD modeling for Reynolds number equals to 275000 for improved airfoils. Characteristics of primary lift force NACA 4412 was taken from reference [20] in 240000 Reynolds number. Figures (5) to (7) show coefficient charts of predicted aerodynamic loads of improved airfoils from numerical methods of panel and CFD. Since panel methods solved ideal flow equation, it does not consider viscosity impacts in aerodynamic forces, thus, it is not able to predict boundary layer separation and its impacts. In order to solve this problem some researchers analyzed flaws around airfoils through couple viscose-non viscose method (Pramod, 2011). Predicted aerodynamic loads behavior is generally linear by panel method. Also, the calculated drag force by panel method is only the pressure drag value resulted from ideal flow solution, consequently, the calculated drag coefficient of this method is much lower than CDF solution and the real value.

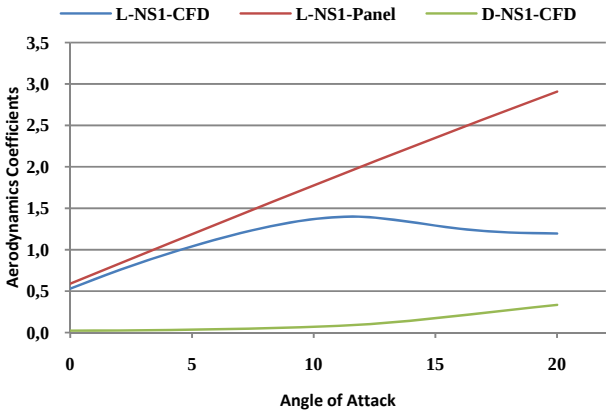

Figure 5. Aerodynamic Loads Coefficients Chart for NS1

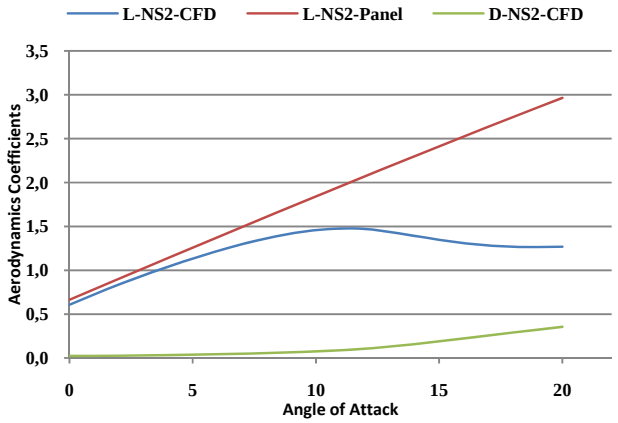

Figure 6. Aerodynamic Loads Coefficients Chart for NS2

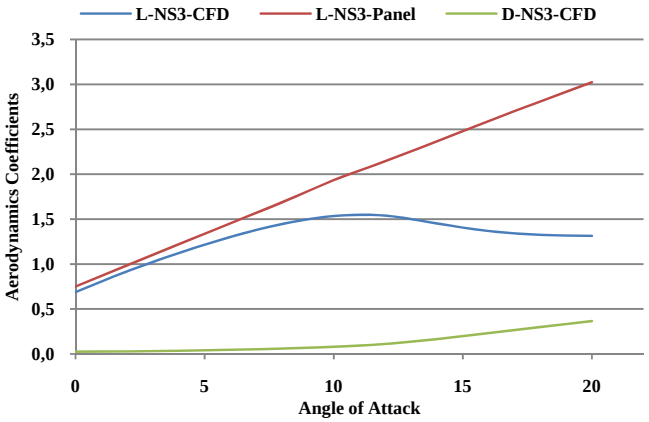

Figure 7. Aerodynamic Loads Coefficients Chart for NS3

Lift coefficient in low angles of attack (lower than 5 degree) with a little difference is similar for the two methods, but after that, results of panel method still continue its linear behavior with too much tilt, though CDF results indicates non-linear behavior. Overall, by increase in angle of attack, the calculated lift coefficient difference through panel and CDF methods increases and panel method is not practically efficient. Results of CDF predict boundary layer separation start from Trailing edge around 9 degree angle of attack for the three designs. Boundary layer separation is created because of inverse pressure gradient and its result is stall phenomenon. In this state lift force reduces severely and creates a turbulent and rotational sequel. The blade flow is severely instable in this area and behavior of aerodynamic forces on the airfoil blade is non-linear (Li, et al. 2013).

Figure (8) shows comparative chart of lift coefficient for primary geometry NACA 4412 and new improved airfoils. With regard to chart lift coefficient in all angles of attack for new airfoils is obviously more than primary airfoils. In the meanwhile, NS3 has the highest lift coefficient.

Spalart-Allmaras predicted stall area and or a little change in upper geometry cause a different behavior in the stall area between primary airfoil and the designed airfoils. However, empirical studies in wind tunnel can analyze Spalart-Allmaras model accuracy in this area. One of the basic parameters in designing wind turbine airfoil is the ratio of lift to drag. Figure 9 shows the chart of lift coefficient in the drag coefficient function (Pramod, 2011). Regarding figure 9, drag coefficient maximum for new airfoils is more than primary airfoils but in similar drag coefficients,

new airfoils have higher lift coefficients. Obviously, the highest lift coefficient in a constant drag coefficient is NS3. In this case, the ratio of lift to drag for this airfoil is more than others.

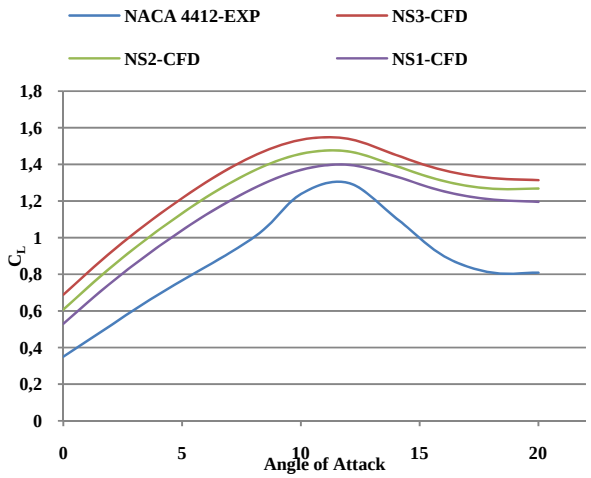

Figure 8. Comparative Chart of Lift Coefficient

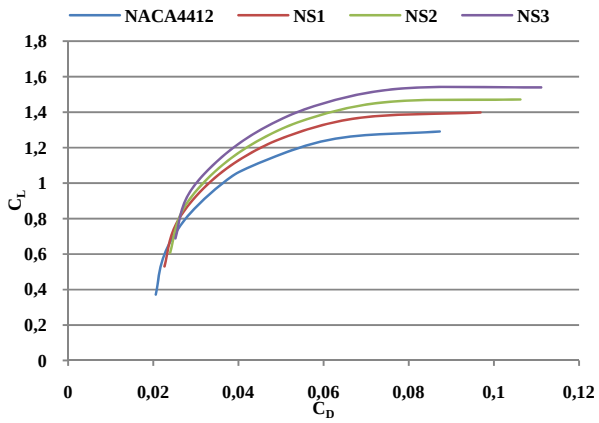

Figure 9. Chart of Lift Coefficient as a Function of Drag Coefficient

Since necessary conditions for airfoils of horizontal axis wind turbines working in low Reynolds numbers and low-speed winds is high lift coefficient and appropriate lift to drag ratio, all improved airfoils of NACA 4412 in this research have better conditions to use in wind turbines with low-speed winds. However, as it was meant in reverse design, by defining speed distribution with higher lift coefficient prediction, NS3 show the best performance among other airfoils. And then NS1 and NS2 are placed in the next places. The highest proportion of lift to drag in all cases occurs in 4 degree angle of attack. Following that, NS2 and NS1 are in the next places. The highest value of lift to drag proportion in all cases occurs in 4 degree angle of attack and NS3 has the highest value with 1, 32 proportion. The lift coefficient in this state was 1,1225. Also, the highest value of lift coefficient in 12 degree angle of attack for NS3 is 15394. In this state, the ratio of lift to drag is 13856. Figure (10) shows distribution of pressure coefficient on NS3 airfoil level in 4 degree angle of attack derived from CFD model and panel method. It seems in higher flow zones the panel and CDF method predict pressure coefficient near to each other. The highest difference occurs in attack

edge and usually, the panel method predicts pressure coefficient (absolute value) higher than the real value.

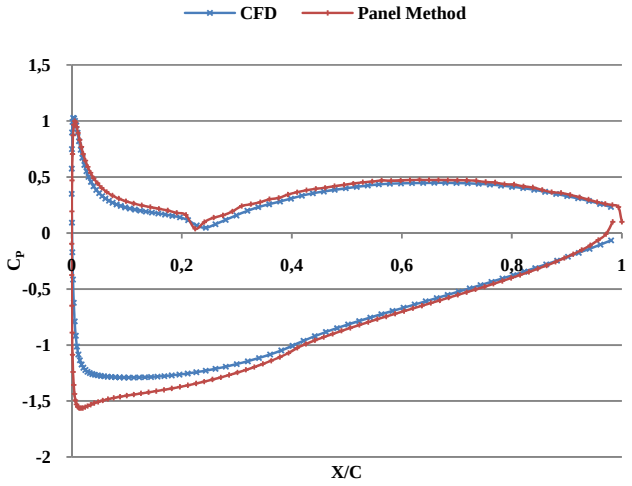

Figure 10. Chart of Pressure Coefficient as A Function Of Chord Percentage In 4 Degree Angle Of Attack

Conclusion

Since horizontal axis wind turbines working in low-speed wind conditions need strong lift force to increase startup torque and appropriate lift to drag ratio for high annual production, NACA 4412 airfoil which is one of common airfoils in using wind turbines by inverse panel was improved to increase lift force. By assuming speed distribution on upper level, three different design of speed distribution was applied by increasing different airfoils to the primary airfoil and three improved airfoils were resulted after a few repetitions. After that, by direct panel method and CDF aerodynamic loads on designed airfoils were predicted. Comparison of results obtained for improved airfoils was conducted with empirical aerodynamic characteristics of primary airfoils and it was determined that lift force in all angles of attack for improved airfoils is more than primary airfoils. In the meanwhile, NS3 had the highest lift coefficient among other designs in similar angles of attack. Also, for stable drag coefficients NS3 represents a higher lift coefficient. The highest ratio of lift to drag coefficient is related to NS3 which occurred at 4 degree angle of attack. CDF predictions refer to boundary layer separation around 9 degree angle of attack for all the three designs. Finally, we found out that NS3 not only perform better than NACA 4412 primary airfoil for using in low-speed wind, but also is more appropriate than two other improved plans. After being confirmed in empirical tests of wind tunnel, research results can help designers in using numerical codes of BEM statement design.

References

Allmaras, S., Johnson. R., Forrester, T., & Spalart, P. R. (2012). Modifications and Clarifications for the Implementation of the Spalart-Allmaras Turbulence Model. 7th International conference on computational fluid dynamics, Big Island: Hawaii.

Babadi Soultanzadeh, M., Mehmandoust Isfahani, & B., Toghrai Semiromi, D. (2014). Numerical Simulation of Flow Field around a Darrieus Vertical Axis Wind Turbine to Estimate Rotational Wake Size. Journal of Middle east applied science and technology, 3 (9).

Bermudez. L, Velazquez, A., & Matesanz, A., (2002). Viscous-inviscid method for the simulation of turbulent unsteady wind turbine airfoil flow, Journal of wind engineering and industrial aerodynamics, 90, 643-661, Elsevier.

Bhutta, M. M., Aslam, H. & Nasir, F. et al. (2012). Vertical Axis Wind Turbine – A Review of Various Configurations And Design Techniques. Elsevier, Renewable and Sustainable Energy Reviews, 16, 1926-1939.

Crivellini, A., D`Alessandro, V. (2014). Spalart-Allmaras Model Apparent Transition And RANS Simulations Of Laminar Separation Bubbles On Airfoils. Elsevier, International journal of heat transfer and fluids flow, 47, 70-83.

Crivellini, A., D`Alessandro, V., Bassi, F., (2014). A Spalart-Allmaras Turbulent Model Implementation In A Discontinues Galerkin Solver For Incompressible Flows. Journal Of Computational Physics, Elsevier, 241, 388-415.

Deck, S., Duveau, P., d`Espiney, P., & Guillen, P. (2002). Development and Application of Spalart-Allmaras One Equation Turbulence Model To Three-Dimensional Supersonic Complex Configurations. Elsevier, Aerospace Science and technology, 6, 171-183.

Drela, M. (n.d.). MIT university, http://web.mit.edu/drela/Public/web/xfoil/.

Henriques, J. C. C., Marques da Silva, F., Estanquerio. A. I, & Gato. L. M. C. (2009). Design of a New Urban Wind Turbine Airfoil Using A Pressure-Load Inverse Method. Elsevier, Renewable Energy, 34, 2728-2734.

Kamoun, B., Afungchui, D., & Chauvin. A. (2005). A Wind Turbine Blade Profile Analysis Code Based On the Singularities Method. Elsevier, Renewablae Energy, 30, 339-352.

Kang, C., Yang, X., & Wang, Y., (2013). Turbulent flow characteristics and dynamics response of a vertical axis spiral rotor, Energies, 6, 2741-2758, MDPI.

Katz, J. & Plotkin, A. (1991). Low Speed Aerodynamics. McGraw-Hill.

Li, C., Zhu, S., Xu, Y., & Xiao, Y. (2013). 2.5D Large Eddy Simulation of Vertical Axis Wind Turbine In Consideration Of High Angle Of Attack Flow. Elsevier, Renewable Energy, 51, 317-330.

Moran, J. (1984). An Introduction to Theoretical and Computational Aerodynamics. Dover Publication.

Pinkerton, R. M. The Variation With Reynolds Number Of Pressure Distribution Over An Airfoil Section. Naca report, 63.Bermudez, L., Velazquez, A., & Matesanz, A. (2002). Viscous-Inviscid Method for the Simulation of Turbulent Unsteady Wind Turbine Airfoil Flow. Elsevier, Journal of wind engineering and industrial aerodynamics, 90, 643-661,

Pramod, J. (2011). Wind Energy Engineering. McGraw-Hill.

Pramod, J. (2011). Wind Energy Engineering. McGraw-Hill.

Rajakumar, S., & Ravindran, D. (2012). Iterative Approach For Optimizing Coefficient Of Power, Coefficient Of Lift And Drag Of Wind Turbine Rotor. Elsevier, Renewable energy, 38, 83-93.

Ravi, H. C., Madhukeshwara, N., & Kumarappa, S. (2013). Numerical Investigation of Flow Transition For NACA 4412 Airfoil Using Computational Fluid Dynamics. International Journal of Innovative Research in Science, Engineering and Technology 2(7), 2778-2785.

Singh. R. K., Rafiuddin Ahmed, M., Asid Zulla,. M., & Lee. Y. H. (2012). Design of A Low Reynolds Number Airfoil For Small Horizontal Axis Wind Turbines. Elsevier, Renewable Energy, 42, 66-76.

Tangler, J. L., & Somers, D. M., (1995). NREL Arifoil Families for HAWTs. National Renewable Energy Laboratory, Colorado: USA.

Yao, J. Y., Weibin, W., Jianliang, Xie. J., Zhou. H., Peng. M., Sun, Y., (2012). Numerical Simulation of Aerodynamic Performance For Two Dimensional Wind Turbine Airfoils. Elsevier, Energy Procedia, 31, 88-86.